



CHORUS

This is the accepted manuscript made available via CHORUS. The article has been published as:

Surface-plasmon-polariton-assisted dissipative backaction cooling and amplification

Iman Hassani nia and Hooman Mohseni

Phys. Rev. A **92**, 053852 — Published 23 November 2015

DOI: [10.1103/PhysRevA.92.053852](https://doi.org/10.1103/PhysRevA.92.053852)

Surface Plasmon Polaritons Assisted Dissipative Back-action Cooling and Amplification

Iman Hassani nia and Hooman Mohseni*

Bio-Inspired Sensors and Optoelectronics Laboratory (BISOL), EECS Department, Northwestern University, Evanston, Illinois, 60208 USA

We evaluate a new method, based on the near-field properties of surface plasmon polaritons, to significantly enhance the dissipative optomechanical backaction mechanism. Although the large momentum of the surface plasmon polariton modes leads to the enhanced sensitivity of the scattering to the mechanical displacement, the overall efficiency will not improve unless an optical antenna efficiently couples the plasmonic modes to the far-field. The predicted improvements in both efficiency and bandwidth make this approach uniquely suitable for many new applications.

PACS numbers: 42.50.Ct, 42.50.Pq, 62.20.D-, 42.50.Wk

The interaction of an optical mode and a mechanical mode within an optical cavity, known as *dynamical backaction*[1, 2], has been always at the center of attention for ultrasensitive measurement and manipulation of the mechanical displacement and force[3, 4]. Significant progress in this field has made it possible to probe the non-classical nature of both photons and phonons[5] leading to the observation of quantum coherence and entanglement[6-9]. Non-equilibrium cooling by backaction optomechanics close to the ground state of vibration can be used for force measurements with precisions beyond the standard quantum limit[10]. Furthermore, due to the Kerr nonlinearity in these optomechanical systems, quantum non demolition (QND) measurements can be made possible[11].

The dynamical backaction is achieved when the displacement of some cavity components changes the optical energy within the cavity. The change of optical energy results in a corresponding exertion of optical force on the moving object, which when in correct phase, exchanges the energy between the optical and mechanical modes. This method has been proposed and used for a broad range of applications ranging from gravitational wave detection[12], to photonic clocks[13], high precision accelerometers[14], atomic force microscopy[15], laser cooling[16, 17] and parametric amplification[18]. The coupling of the mechanical mode to the optical cavity can be either dispersive or dissipative. In the dispersive coupling, the mechanical motion changes the optical energy by altering photons' phase and the interference between them inside the cavity. It has been shown that the dispersive backaction coupling can be employed to annihilate the phonons completely in the “good cavity limit”[19,

20] (also known as “resolved side band regime”[20]) for reaching the ground state of vibration . In the good cavity limit the mechanical vibration frequency is much larger than the photon damping rate (κ), resulting in sufficient phase matching of the optical force for the efficient cooling. However, achieving this condition is quite challenging and requires fabrication of cavities with very high quality factors that limits its practical implementation for many sensing applications. Even if such cavities are perfectly fabricated, the cavity quality factor (Q_o) is prone to change by the environmental conditions (for instance when used as a biosensor it can be affected by the micro fluidic channel and the scattering induced by the surrounding particles[21]). On the other hand a very high optical quality factor necessitates the use of an ultra-narrowband laser beam which is accurately detuned from the cavity resonance frequency (f_o) by the mechanical vibration frequency (f_m)[18]. These ultra-narrowband lasers with fine tuning capability add to the cost of the total system. Furthermore the narrowband nature of this technique is a limitation that prevents its application for broadband detection and sensing of molecules. The alternative approach is the dissipative backaction mechanism[3] in which the mechanical displacement changes the optical energy of the cavity by changing the photons’ damping rate. This technique has been theoretically predicted[3] and experimentally verified by a vibrating ridge waveguide coupled to a microdisk cavity[22] and a fiber taper waveguide coupled to nano-cavity formed between the two suspended cantilevers[23, 24] that has the capability of both dissipative and dispersive coupling[23] . In contrast to the dispersive coupling, ground state cooling can be achieved even without being in the good cavity limit[3]. Although this outstanding feature alleviates the stringent requirement for the cavity quality factor, however the change in the photon damping rate due to the motion should be large enough to have a significant mechanical damping for ground state cooling[3, 23]. In this Letter, we discuss the potential of surface plasmon polaritons for significant enhancement of the dissipative coupling. The work described here is motivated by recent demonstration of unique properties of surface plasmon polaritons for nanoscale optical transduction[25]. We present an in-depth inspection of various physical properties of surface plasmon polaritons to realize cavity backaction optomechanical devices with significantly lower optical quality factors that are efficient, compact and broadband.

To see whether plasmonic structures can be useful for this purpose, we start by recalling that the mechanical damping rate can be calculated as[3]:

$$\gamma_{opt} = B^2 \bar{n} \kappa \frac{\omega_m^2}{[3\omega_m / 2 + (A/B)\kappa]^2 + \kappa^2 / 4}, \quad (1)$$

which is equal to the mechanical damping rate of the cavity when the dissipative optomechanical interaction is dominant. Such scheme is an alternative for the more popular sideband-resolved laser cooling regime that makes exclusive use of dispersive coupling. The above expression is valid at optimum detuning, i.e ($\Delta_{opt} = \omega_m / 2 + (A/B)\kappa$, where $\omega_m = f_m / (2\pi)$ and κ and \bar{n} are

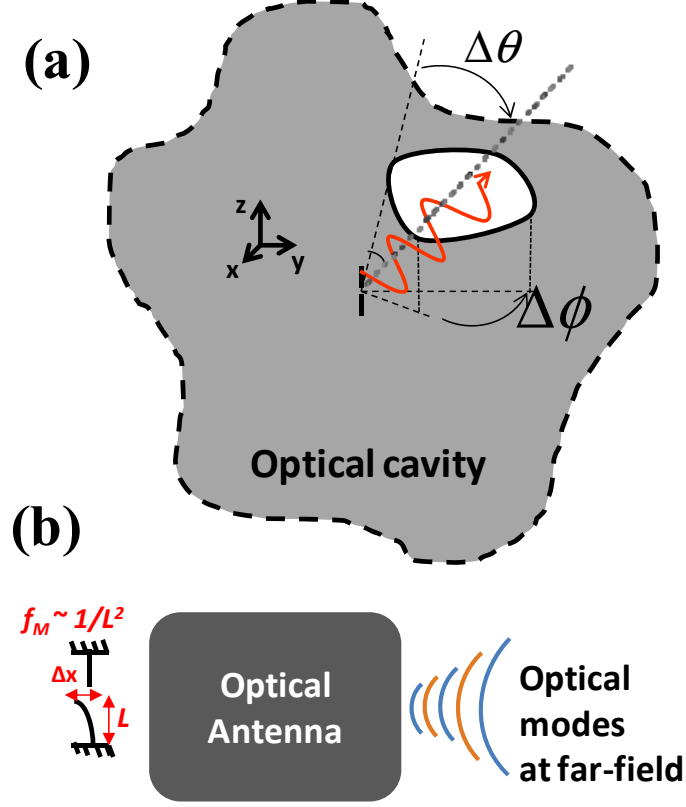


FIG. 1 (a) Schematics of a plasmonic structure which scatters photons out of the cavity through a fictional aperture in the far field at the cavity wall. The aperture covers a polar angle range ($\Delta\theta$) and an azimuthal angle range ($\Delta\phi$) with respect to the center of the plasmonic structure. The numerical aperture of the fictional aperture is defined as $n\sin(\Delta\theta)$ (b) Schematics of the plasmonic optomechanical coupling to far-field modes. While the mechanical frequency of vibration increases with the reduction of the length as $\sim 1/L^2$, coupling to the structure decreases linearly. An optical antenna can significantly enhance the weak coupling of sub-wavelength plasmonic optomechanical structures to the far-field modes.

the damping rate and the average number of photons inside the cavity respectively. A and B are the dispersive and dissipative coupling coefficients[3]. The phonon number at equilibrium ($n_{ph} = (\gamma_m / (\gamma_{opt} + \gamma_m))n_{eq}$ where γ_m is the mechanical damping rate and n_{eq} is the phonons occupation number governed by Bose-Einstein distribution function) can be lowered by maximizing the optically induced damping rate. In this respect, the damping rate per photon number inside the cavity can be used as a figure of merit. In previous attempts[22, 26], the best structure for dissipative cooling consisted of an ultrahigh quality disk resonator coupled to a suspended ridge waveguide.

Looking back at Eq.(1), the denominator indicates that the photon damping rate should be kept as low as possible to maintain the cavity feedback mechanism and prevent substantial loss

of optical energy in the system in order to achieve a high efficiency. On the other hand, in order to increase the numerator both the mechanical vibration frequency and the dissipative coupling coefficient i.e. $B = (x_{zpt} / \kappa)(d\kappa / dx)$, should be increased. Consequently both the relative change of damping rate versus position and the zero point fluctuation amplitude (x_{zpt}) should be maximized. It should be noted that the dispersive coupling coefficient for a cavity with optical radial resonance frequency of ω_R , is equal to $A = (x_{zpt} / \kappa)(d\omega_R / dx)$ and should be minimized to have maximum dissipative cooling and amplification. In the example that we shall work out later, the dispersive coupling for the lateral motion of the plasmonic structure is negligible compared to the dissipative coupling.

The change of photon decay rate versus position is usually achieved by changing the transmission through one of the cavity ports upon motion. The change in the transmission can be enhanced by using highly confined surface plasmon polaritons (SPPs) with large wavevectors. Recent experimental observation of large dispersive optomechanical coupling in a nano-plasmonic structure [25] suggests a potential for achieving similarly large dissipative coupling. This could be achieved for instance by introducing a plasmonic resonator with mechanical degrees of freedom that would mediate power out-coupling from a dielectric optical resonator. Moreover, the sub-wavelength nature of SPPs can be exploited to design plasmonic structures with smaller dimensions. The benefits are twofold: First, the fundamental resonance frequency of the mechanical oscillation can be increased significantly, since it is inversely proportional to the square of the dimension ($f_m \propto 1/L^2$). Second, the zero point fluctuation amplitude $x_{zpt} = \sqrt{\hbar / (2m_{eff}\omega_m)}$ is enhanced due to the reduction of the effective mass ($m_{eff} \propto L^3$).

Despite the above benefits, there are two main challenges associated with the use of plasmonic structures: (1) plasmonic materials introduce loss and increase the damping rate of the cavity, which opposes the enhancement of γ_{opt} . Although the increase in loss might be desirable for applications where a more broadband cavity and less sensitivity to laser line-width and detuning are required, the large magnitude of the loss prevents the use of purely SPP backaction mechanism in plasmonic cavities due to very short SPP lifetime. In this case, heating the mechanical oscillator caused by the metal loss is negligible due to the large thermal conductivity of the metal as shown by previous experimental and theoretical studies[27, 28] (2) Small structures with large mechanical oscillation frequencies containing highly confined plasmonic modes suffer from weak coupling to the far-field. To illustrate the latter issue, consider a sub-wavelength structure within an arbitrary cavity as depicted in Fig. 1(a). In this case, we assume that the decay rate of the cavity optical energy is dominated by the power flow through a fictional aperture in the far field of the plasmonic structure which mediates the power out-coupling. The mechanical movement of the plasmonic components would result in the change of its scattering properties and hence the optical power exiting the cavity and the photon damping rate. Since the

dimensions of the plasmonic structures of interest are going to be smaller than the free-space wavelength, an “optically small” dipole will be a good representative. The re-radiated power from this structure is equal to $(\frac{\pi}{3})Z\left|\frac{I_0L}{\lambda}\right|^2$ [29, 30], where I_0 is the induced current within, and L is the length of the subwavelength dipole and Z is the vacuum impedance. The induced current is equal to the displacement current with the magnitude equal to $\omega\epsilon_m E_m$, where ϵ_m is the electric permittivity and E_m is the magnitude of the electric field in the metal[31]. The fraction of the reradiated (scattered) power which reaches the aperture is equal to $(1/P_{total})\iint\frac{cn\epsilon_0}{2}E_p^2r^2\sin(\theta)d\theta d\phi$ where P_{total} is the total power emitted by the dipole, n is refractive index of the cavity medium, ϵ_0 is the dielectric permittivity of vacuum, E_p is the magnitude of the electric field of the wave emitted by the dipole at far-field and the integration is carried out within the polar and azimuthal angle of the aperture as shown in Fig. 1(a). Using the farfield distribution of a sub-wavelength dipole, the total power reaching the aperture through scattering is found to be:

$$P_{out} = \left(\frac{1}{3\pi}\right)Z\left|\frac{I_0L}{\lambda}\right|^2 \{2\sin^{-1}(NA/n) - \cos(2\theta_0)\sin[2\sin^{-1}(NA/n)]\}\sin^{-1}(NA/n), \quad (2)$$

where n is the index of the refraction of the cavity, θ_0 is polar angle of the center of the aperture and NA is defined as $n\sin(\Delta\theta/2)$ where $\Delta\theta$ is the polar angle range of the rays reaching the aperture [see Fig. 1(a)]. It is evident from the above equation that the reradiated power (and the coupling to the far field) is proportional to the square of the structure dimension (L^2). A similar conclusion is reached when dealing with a sub-wavelength plasmonic aperture, which has a radiation intensity proportional to the square of its dimensions[32].

Consider that a resonant cavity mode interacts with the plasmonic structure within the dielectric cavity as shown in Fig.1 (a). The resonant cavity mode can be regarded as a Gaussian beam close to the subwavelength plasmonic structure. Furthermore, as we stated before, a dipole antenna as a basic optical element can be considered to represent the subwavelength plasmonic structure. To have maximum coupling, we assume that the dipole antenna is placed at the high field intensity point of the Gaussian cavity mode. In this case, according to Eq .2, the overlap of the dipole radiation pattern and the optical mode in the far-field, increases by increasing the NA of the optical mode. Although for high NA cavity modes this implies a high coupling, the photon lifetime does not change considerably with small mechanical reconfigurations of the dipole antenna. This is because the change in the overlap integral of the far-field pattern of the dipole antenna and the cavity mode profile (that covers a large solid angle) is essentially small. Consequently, another fundamental limitation is that the increase in the far-field coupling (by increasing the NA of the incident beam) results in the decrease of the change in the photon

lifetime and the dissipative optomechanical interaction. To summarize, in order to achieve the benefits of the subwavelength plasmonic structures to the fullest extent, the following conditions should be met: (1)- The photon damping rate should be determined by scattering from the plasmonic structure within the cavity. (2)- By integrating the plasmonic structures to high Q optical cavities, sufficiently low damping rates should be maintained. (3)- Good couplings to subwavelength plasmonic structures(with large acceptance cones) without sacrificing the dissipative coupling is required. As we shall see in the following “near-field coupling” can be employed for this purpose.

By using coupled mode theory (CMT), Karalis et al[33] has theoretically shown that the near-field coupling leads to very efficient energy transfer between two media which are only a few wavelengths apart. This efficient near-field coupling might provide an excellent alternative approach. However, to improve the coupling using this method, most of the cavity energy should be localized at the near field of the plasmonic structure. Two good examples are the coupling between the microspheres in a chain[34] and the coupling to a plasmonic waveguide structure using a taper coupler[35]. In both examples, not only is the light focused at the interface (enhanced localization) but also the coupling can be significantly enhanced through the nonradiative near field channel[34]. These examples show the many possibilities in enhancing the coupling through near field. We consider a mediating antenna that can increase the optical cross section (as seen by the aperture) of the sub-wavelength plasmonic structure through near field coupling as shown in Fig. 1(b). The “near-field coupling” here is basically the same as what has been generally defined as the rate of energy transfer between the two optical modes of two objects located in the near-field of each other [35]. The transferred power can be scattered by the plasmonic structure leading to the change of the photon lifetime within the whole system. The near-field coupling as described by the coupled mode theory (CMT) can be expressed by $(\omega_1 / 2) \int d^3r \epsilon_2(r) E_2^*(r) E_1(r) / \int d^3r \epsilon(r) |E_1(r)|^2$ where ω_i , ϵ_i , E_i are the resonance frequency, the electric permittivity and the electric field eigen-mode of the i^{th} structure ($i=1,2$) respectively, r is the position and ϵ is the electric permittivity of the medium with the presence of both structures. It should be noted that based on the above formula the amount of near field coupling depends on the structures’ geometrical properties as well as the distance between them and the refractive indices. Therefore, no analytical formula exists that can be applied in a general manner as in the case of far-field coupling [see Eq.(2)]. We mention that, as opposed to far-field coupling which decreases by the square of the plasmonic structure dimensions [see Eq.(2)], the near field coupling can be quite large as long as the electric field overlap integral of both structure remains large. In fact, as suggested in Ref [35], the subwavelength structures with long evanescent field tails, can have large near field couplings over longer separation distances. Now suppose that the second medium is the optical cavity that can sustain photons with a long lifetime. By optimizing the structural parameters (as we demonstrate in our example) a good near field coupling between the cavity mode and the subwavelength plasmonic structure can be obtained. Furthermore since it is a near-field coupling, it can be quite sensitive to the mechanical reconfiguration of the

plasmonic structure which in turn changes the photon lifetime of the optical cavity. As a result, a significantly enhanced dissipative optomechanical interaction by the virtue of both high quality factor of the optical cavity and the large optomechanical transduction properties of subwavelength plasmonic structure could be achieved.

Here, we present our simulations for near-field to far-field coupling through a microsphere optical cavity. While taking advantage of plasmonic properties, such a hybrid opto-plasmonic cavity would also alleviate the adverse effect of plasmonic loss on the photon lifetime by providing a long photon roundtrip inside the microsphere optical cavity. As our simulations predict in the following, with a good trade-off between all of the aforementioned parameters, the proposed plasmonic structure can outperform the best structures reported so far for the purpose of dissipative optomechanical interaction.

The schematic of the hybrid plasmonic microsphere cavity is shown in Fig. 2. The microsphere cavity sits on top of a perfect Distributed Bragg Reflector (DBR). Top of the microsphere is covered by aluminum to form the hybrid cavity. Among all of the metals,

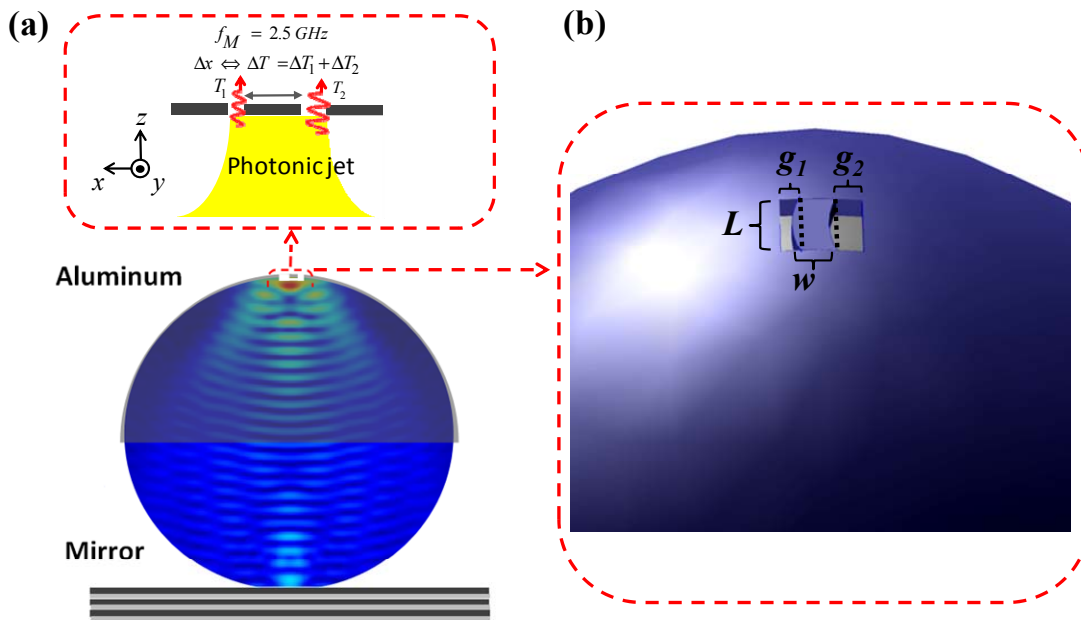


FIG. 2 (a) The schematics of the simulated microsphere cavity with the asymmetric metal insulator metal structures fabricated on top and center of the sphere. A magnified cross section view of the asymmetric plasmonic structure is also provided. The lateral motion of the suspended beam (with mechanical frequency $f_M = 2.5$ GHz) results in the change of transmission (ΔT) through the plasmonic cavities and the photon lifetime within the whole structure. (b) The mechanical mode profile of the lateral flexural vibrations. The edges of the nano-beam at its equilibrium position are also shown by the dotted lines. The asymmetry is necessary to achieve a significant change of transmission and dissipative interaction with very small lateral vibrations of the nano-beam. The beam width (w), length (L) and the gap widths (g_1 and g_2) are given in the text.

aluminum has the best properties due to its lower mass density (and consequently lower effective mass of the suspended beam), high Young's modulus and relatively low-loss. A suspended plasmonic beam with the length (L) of 500 nm is carved out of aluminum at the very top of the microsphere (see the magnified view of the plasmonic structure in Fig. 2). There are two apertures on the sides of the plasmonic beam with different widths ($g_1=50$ and $g_2=80$ nm) to have nonzero dissipative coupling with the first lateral flexural motion of the beam. The mechanical modes of the structures were solved for using a commercial finite difference solver and the profile of the mechanical motion is shown in Fig. 2. A comparison to the schematics of Fig. 1 helps to have a better understanding of the introduced mechanisms. The microsphere cavity is the optical cavity of Fig.2 that contains the nano-beam plasmonic structure. However unlike Fig.2 which shows that the plasmonic structure is located in the far field of the exit-aperture, here it is in the near field of the aperture. On the other hand, the microsphere acts as a dielectric antenna[36, 37] placed at the near-field of the plasmonic structure[38] to increase the optical cross section of the plasmonic structure. As illustrated in Fig. 1(b), this helps to increase the coupling to subwavelength structures. Consequently, both the coupling to the plasmonic structure and the coupling to the exit-aperture through the plasmonic structure are provided by the near-field interaction. The sphere optical cavity has a good quality factor even with the presence of the aperture and the damping rate of the system is critically dependent on the mechanical state of the plasmonic nano-beam. As a result, all of the three introduced issues for the use of subwavelength plasmonic structures can be addressed in the introduced structure.

In order to find the optomechanical cooling and amplification rates for the lateral vibrations, we simulated the structure using commercial finite difference time domain software

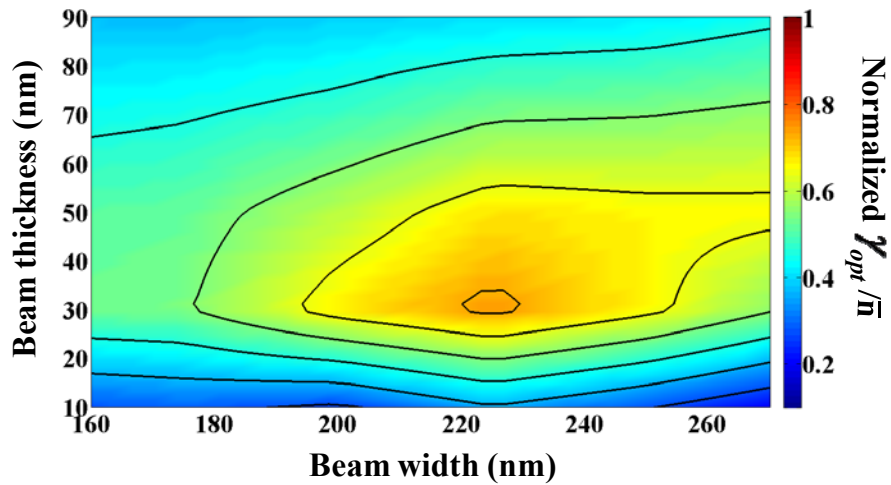


FIG. 3 The dissipative damping rate per trapped photon versus the suspended beam width and the beam thickness (in this case, it is equal to the aluminum thickness).

and the results have been shown in Fig. 3. We performed a series of static simulations with varying nano-beam positions to find $d\kappa/dx$. We then used $d\kappa/dx$ to find the dissipative optomechanical coefficient (B) and the dissipative damping rate (γ_{opt}) as expressed by Eq.(1). As the suspended beam becomes wider than the width of the focused light, the coupling through the slots decreases. On the other hand for very small beams, the effect of the beam movement on the optical properties of the asymmetric slot structure diminishes. Consequently, there is an optimum beam-width for the optomechanical damping rate as can be seen in Fig. 3. The thickness of the metal determines the effective plasmonic cavity length that is formed between the two metal-air interfaces at the bottom and on top of the slots. Therefore, at a particular value it results in the maximum change of damping rate with the lateral motion for the narrowband light. According to Fig. 3, we found the optimized values for the beam width ($w=225$ nm) and the beam thickness ($t=30$ nm) and used those values for the results presented in Table I. We have assumed that the microsphere is placed on top of a single moded fiber (at 1550 nm) to form a fiber-integrated plasmonic device. It should be noted that we have been recently made a similar structure with a plasmonic antenna on the top and center of a microsphere that was placed on an optical fiber facet[39]. Our results show that the photon reflection from the two slots at the top is the dominant factor that limits the quality factor of the microsphere cavity (Q) and the loss due to

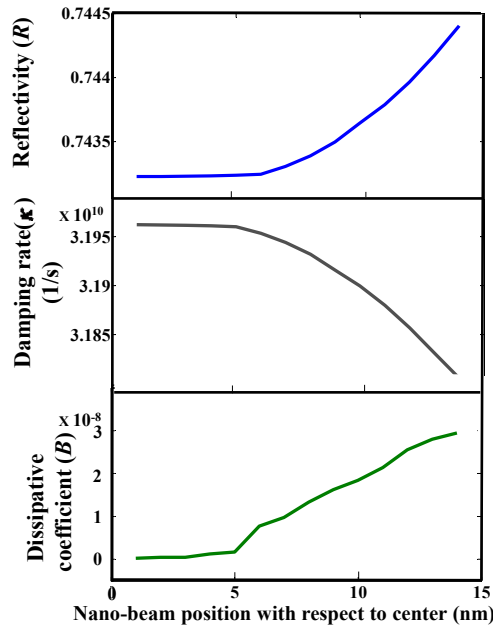


FIG. 4. The simulated reflectivity of the photonic nanojet off the plasmonic beam (R), the corresponding damping rate (Γ) and dissipative coupling coefficient (B) versus the lateral position of the optimized suspended nano-beam. It is evident that when the nano-beam is fabricated exactly in the middle, with both slots having the same width, the change in the beam reflectivity versus the lateral displacement and the corresponding dissipative coupling coefficient vanishes due to the symmetry.

diffraction is insignificant compared to the reflection loss from the metallic structure. The dispersion relation for different slot widths has been calculated in Ref [25]. As the slot width decreases the dispersion curve bends and deviates from the light line. For narrower slots, the change in the wavevector per unit change in the slot width is higher [25]. As the nano-beam moves away from the center, one of the slots becomes wider allowing more photons to transmit while the other one gets narrower and blocks the light transmission. Based on the dispersion curves, the increase in the momentum mismatch for the narrower slot is higher compared to its reduction for the wider slot. On the other hand, the variation in the intensity of the photonic jet is negligible across the subwavelength plasmonic structure. Therefore, the overall coupling and transmission through the plasmonic structure decreases as the nano-beam is positioned away from the center leading to the increase in the reflectivity. This trend can be seen by the numerical results in FIG. 4 which also shows the damping rate and the calculated dissipative coefficient (B) of the optimized structure. The performance metrics can be compared to the microdisk resonator coupled to a

TABLE I. Parameters of different structures utilizing the dissipative optomechanical cooling. Q_m is the mechanical quality factor.

Structure	Properties	Q_o	Q_M	f_m (Hz)	f_o (Hz)	m_{eff} (Kg)	$d\kappa/dx$ (MHz/nm)	κ (Hz)	γ_{opt}/\bar{n} (Hz)
Our proposed plasmonic device (d=120 μm) with perfect DBR		6×10^3	$10^2 \sim 10^{3a}$	2.5×10^9	1.95×10^{14}	2.9×10^{-17}	35.24	3.2×10^{10}	5×10^{-6}
Vibrating ridge waveguide coupled to a disk resonator ^b		1.2×10^5	5×10^3	2.5×10^7	2×10^{14}	9.18×10^{-16c}	26	1.67×10^9	5×10^{-6d}
Vibrating ridge waveguide coupled to a disk resonator ^e		5.91×10^6	5×10^4	1×10^7	3.55×10^{14}	5×10^{-16}	≤ 0.2	6×10^7	1.7×10^{-7f}
Fiber taper coupled to split-beam photonic crystal nano cavity ^f		5.2×10^3	2.4×10^{3g}	1.05×10^7	1.97×10^{14}	$> 3.48 \times 10^{-16}$	~ 2	3.8×10^{10}	2.8×10^{-12h}

^a The range of the mechanical quality factor is estimated based on the values found in literature[40, 41].

^b Reference[22].

^{c,d,f,h} These values were calculated based on the data provided in the references.

^e Reference[26].

^f Reference[23].

^g extracted from Ref[24] which similar mechanical structure as in Ref[23].

suspended waveguide as reported by the references included in Table I. The interacting optical mode inside the microsphere cavity is like a Fabry-Perot mode. It starts from the DBR side of the cavity with almost the same profile of the exiting beam of a single-moded fiber (a Gaussian beam with effective mode diameter of almost 9 μm) and is gradually focused to the other end of the microsphere where the plasmonic structure is located. Upon reflecting back from the structure, it travels the same path to reach the DBR mirror. To confirm that the mode is indeed like a Fabry Perot mode of an elaton, we calculated the cavity damping rate for different diameters of the microsphere and with different reflectivities of the plasmonic structure by using two different types of simulations. In the first method, the damping rates were obtained by our FDTD simulations using multiple point monitors within the microsphere cavity that give the decay of the resonant field components over time. Then, we performed another type of FDTD simulation in which the plasmonic devices were excited by the same cavity mode source but without the Bottom DBR mirror. The latter simulation gave us the effective reflectivity of the aluminum mirror comprising the plasmonic structure (R_I). We could verify the following well-established formula of a Fabry-Perot cavity:

$$\kappa = -c / (nL_{eff}) \ln(R_1 R_2) \quad (3)$$

Where κ is the damping rate, n is the refractive index of the cavity (equal to 2 in our simulations), R_2 is the reflectivity of the DBR mirror and L_{eff} is the effective length of the Fabry-Perot cavity. The results of our second simulation of reflectivity were employed to calculate κ using the above formula. These results are in excellent agreement with the direct calculations based on time monitors (first simulation) when L_{eff} is 20 percent larger than the diameters of the simulated microspheres. The dielectric microsphere is a practical structure that can focus light into a beam known as photonic nanojet, which is an elongated beam that is about one wavelength long and has a width of about one third of the wavelength[42]. We have previously shown that formation of photonic nanojet helps increase the optical intensity and coupling to the near-field modes[43]. From Table I, it can be seen that the quality factor of the proposed structure is significantly smaller, however the enhancement of dissipative coupling coefficient, mechanical resonance frequency and the reduction of the effective mass is evident. Consequently, the proposed structure has a damping rate per phonon number (γ_{opt} / \bar{n}) that reaches those of the best reported structures. It is worth mentioning that in the absence of the enhanced mode coupling produced by the microsphere, the damping rate per phonon number for the bare plasmonic structure drops by more than three orders of magnitude.

In conclusion, a new class of optomechanical devices based on surface plasmon polaritons is proposed. Unlike existing approaches, a high efficiency can be achieved over a broad optical bandwidth. A specific example with a simple plasmonic structure was provided to demonstrate that an induced damping rate per phonon number as high as the best reported structures is possible over ~ 20 times broader bandwidth. The increase in the cavity bandwidth (or

the cavity damping rate) reduces the variation of the corresponding cooling rate with respect to the detuning. We start by noting that the cooling rate can be expressed as[3]:

$$\gamma_{opt} = x_{zpt}^2 [S_{FF}(\omega_M) - S_{FF}(-\omega_M)] \quad (4)$$

Where $S_{FF}(\omega)$ is the backaction force noise spectrum and is given by[3]:

$$S_{FF}(\omega) = \kappa \left(\frac{B|a|}{2x_{zpt}} \right)^2 \frac{[\omega + 2\Delta - (2A/B)\kappa]^2}{(\omega + \Delta)^2 + \kappa^2 / 4} \quad (5)$$

For the case of dominant dissipative coupling ($B \gg A$), with laser detuning well within the cavity bandwidth ($\kappa \gg \Delta$) and for sideband-unresolved regime ($\kappa \gg \omega_M$) where the dissipative optomechanical coupling outperforms the dispersive interaction as stated earlier, the cooling rate per one photon becomes approximately equal to $8|B|^2 (\omega_M / \kappa) \Delta$. Therefore, in this case, the relation between the cooling rate and the detuning is linear and the reduction in the damping rate of the cavity steepens the slope of cooling rate. The described conditions necessary to arrive to this linear relation hold for all of the structures listed in Table.I. We found that the slope of the cooling rate versus detuning for the plasmonic structure is almost 20 times smaller than the microdisk structure[22] listed in the second row of Table.I. This example shows that by using plasmonic structures not only the burden of fabricating ultra-high quality cavities can be alleviated but also comparatively large dissipative optomechanical interaction with less sensitivity to the laser detuning can be achieved.

This example is by no means demonstrating the performance limit of the proposed approach, and we believe that more sophisticated and optimized plasmonic structures can be designed with higher efficiency and broader bandwidth.

We would like to acknowledge the partial support from NSF award #ECCS-131062, DARPA award # W911NF-13-1-0485 and ARO award # W911NF-11-1-0390, as well as the support from high performance computational center (QUEST) at Northwestern University.

* hmohseni@eecs.northwestern.edu

- [1] I. Wilson-Rae, N. Nooshi, W. Zwerger, and T. J. Kippenberg, *Physical Review Letters* **99**,093901 (2007).
- [2] V. B. Braginsky, V. B. Braginskiĭ, and F. Y. Khalili, *Quantum measurement* (Cambridge University Press, 1995).
- [3] F. Elste, S. Girvin, and A. Clerk, *Physical Review Letters* **102**,207209 (2009).

- [4] J. Khurgin, M. Pruessner, T. Stievater, and W. Rabinovich, *Physical Review Letters* **108**,223904 (2012).
- [5] y. Leibfried, R. Blatt, C. Monroe, and D. Wineland, *Reviews of Modern Physics* **75**,281 (2003).
- [6] M. Pinard, A. Dantan, D. Vitali, O. Arcizet, T. Briant, and A. Heidmann, *EPL (Europhysics Letters)* **72**,747 (2005).
- [7] S. Mancini, V. Man'ko, and P. Tombesi, *Physical Review A* **55**,3042 (1997).
- [8] W. Marshall, C. Simon, R. Penrose, and D. Bouwmeester, *Physical Review Letters* **91**,130401 (2003).
- [9] A. Armour, M. Blencowe, and K. Schwab, *Physical Review Letters* **88**,148301 (2002).
- [10] I. Wilson-Rae, P. Zoller, and A. Imamoglu, *Physical Review Letters* **92**,075507 (2004).
- [11] K. Jacobs, P. Tombesi, M. Collett, and D. Walls, *Physical Review A* **49**,1961 (1994).
- [12] M. Aspelmeyer, P. Meystre, and K. Schwab, *Physics Today* **65**,29 (2012).
- [13] M. Hossein-Zadeh and K. J. Vahala, *IEEE Journal of Selected Topics in Quantum Electronics* **16**,276 (2010).
- [14] A. G. Krause, M. Winger, T. D. Blasius, Q. Lin, and O. Painter, *Nature Photonics* **6**,768 (2012).
- [15] K. Srinivasan, H. Miao, M. T. Rakher, M. Davanco, and V. Aksyuk, *Nano letters* **11**,791 (2011).
- [16] J. Chan, T. M. Alegre, A. H. Safavi-Naeini, J. T. Hill, A. Krause, S. Gröblacher, M. Aspelmeyer, and O. Painter, *Nature* **478**,89 (2011).
- [17] I. H. Nia and H. Mohseni, *Applied Physics Letters* **105**,042102 (2014).
- [18] T. J. Kippenberg and K. J. Vahala, *Optics Express* **15**,17172 (2007).
- [19] F. Marquardt and S. M. Girvin, *arXiv preprint arXiv:0905.0566* (2009).
- [20] T. J. Kippenberg and K. J. Vahala, *Science* **321**,1172 (2008).
- [21] K. H. Kim, G. Bahl, W. Lee, J. Liu, M. Tomes, X. Fan, and T. Carmon, *Light: Science & Applications* **2**,e110 (2013).
- [22] M. Li, W. H. Pernice, and H. X. Tang, *Physical Review Letters* **103**,223901 (2009).
- [23] A. C. Hryciw, M. Wu, B. Khanaliloo, and P. E. Barclay, *Optica* **2**,491 (2015).
- [24] M. Wu, A. C. Hryciw, C. Healey, D. P. Lake, H. Jayakumar, M. R. Freeman, J. P. Davis, and P. E. Barclay, *Physical Review X* **4**,021052 (2014).
- [25] R. Thijssen, E. Verhagen, T. J. Kippenberg, and A. Polman, *Nano letters* **13**,3293 (2013).
- [26] G. Anetsberger, E. Gavartin, O. Arcizet, Q. P. Unterreithmeier, E. M. Weig, M. L. Gorodetsky, J. P. Kotthaus, and T. J. Kippenberg, *Physical Review A* **82**,061804 (2010).
- [27] C. H. Metzger and K. Karrai, *Nature* **432**,1002 (2004).
- [28] C. Metzger, I. Favero, A. Ortlieb, and K. Karrai, *Physical Review B* **78**,035309 (2008).
- [29] M. Agio, *Nanoscale* **4**,692 (2012).
- [30] S. R. Best and B. C. Kaanta, *Antennas and Propagation Magazine, IEEE* **51**,26 (2009).
- [31] A. Alù and N. Engheta, *Physical Review Letters* **101**,043901 (2008).
- [32] C. A. Balanis, *Antenna theory: analysis and design* (John Wiley & Sons, 2012).
- [33] A. Karalis, J. D. Joannopoulos, and M. Soljačić, *Annals of Physics* **323**,34 (2008).
- [34] Z. Chen, A. Taflove, and V. Backman, *Optics Letters* **31**,389 (2006).
- [35] P. Ginzburg, D. Arbel, and M. Orenstein, *Optics Letters* **31**,3288 (2006).
- [36] A. Bonakdar and H. Mohseni, *Optics Letters* **38**,2726 (2013).
- [37] A. Bonakdar and H. Mohseni, *Nanoscale* **6**,10961 (2014).
- [38] D. Gérard, A. Devilez, H. Aouani, B. Stout, N. Bonod, J. Wenger, E. Popov, and H. Rigneault, *JOSA B* **26**,1473 (2009).
- [39] R. M. Gelfand, A. Bonakdar, O. G. Memis, and H. Mohseni, in *SPIE NanoScience+ Engineering* (International Society for Optics and Photonics, 2013), pp. 88150R.
- [40] M. Aspelmeyer, T. J. Kippenberg, and F. Marquardt, *Reviews of Modern Physics* **86**,1391 (2014).
- [41] M. Li, W. Pernice, and H. Tang, *Applied Physics Letters* **97**,183110 (2010).

- [42] A. Heifetz, S.-C. Kong, A. V. Sahakian, A. Taflove, and V. Backman, *Journal of Computational and Theoretical Nanoscience* **6**,1979 (2009).
- [43] H. M. Alireza Bonakdar, *Optics Letters* **38**,2726 (2013).